

Turbulence Structure and Implications for Dispersion: Insights from Large-Eddy Simulations

R. Calhoun, R. Cederwall and R. Street

This article was submitted to
American Meteorological Society
11th Symposium on Global Change Studies
Long Beach, CA
January 9-14, 2000

U.S. Department of Energy

Lawrence
Livermore
National
Laboratory

October 4, 1999

DISCLAIMER

This document was prepared as an account of work sponsored by an agency of the United States Government. Neither the United States Government nor the University of California nor any of their employees, makes any warranty, express or implied, or assumes any legal liability or responsibility for the accuracy, completeness, or usefulness of any information, apparatus, product, or process disclosed, or represents that its use would not infringe privately owned rights. Reference herein to any specific commercial product, process, or service by trade name, trademark, manufacturer, or otherwise, does not necessarily constitute or imply its endorsement, recommendation, or favoring by the United States Government or the University of California. The views and opinions of authors expressed herein do not necessarily state or reflect those of the United States Government or the University of California, and shall not be used for advertising or product endorsement purposes.

This is a preprint of a paper intended for publication in a journal or proceedings. Since changes may be made before publication, this preprint is made available with the understanding that it will not be cited or reproduced without the permission of the author.

This report has been reproduced
directly from the best available copy.

Available to DOE and DOE contractors from the
Office of Scientific and Technical Information
P.O. Box 62, Oak Ridge, TN 37831
Prices available from (423) 576-8401
<http://apollo.osti.gov/bridge/>

Available to the public from the
National Technical Information Service
U.S. Department of Commerce
5285 Port Royal Rd.,
Springfield, VA 22161
<http://www.ntis.gov/>

OR

Lawrence Livermore National Laboratory
Technical Information Department's Digital Library
<http://www.llnl.gov/tid/Library.html>

2.2 TURBULENCE STRUCTURE AND IMPLICATIONS FOR DISPERSION: INSIGHTS FROM LARGE-EDDY SIMULATIONS

R. Calhoun, R. Cederwall, R. Street*

Lawrence Livermore National Laboratory
7000 East Ave, Livermore CA 94550

*Environmental Fluid Mechanics Laboratory
Stanford University, Stanford CA 94305

1. INTRODUCTION

Dispersion modeling in the atmosphere generally requires some form of input describing the turbulence characteristics of the flow field. In some cases, it is acceptably accurate to assume that the turbulence is homogeneous and isotropic and to utilize dispersion models accordingly. However, it has become clear that there are a variety atmospheric flows where the turbulence is more challenging to characterize.

We argue in the following paper that understanding the fluid mechanical details (as provided through Large-eddy simulations [LES]) will be increasingly useful for improved atmospheric dispersion modeling. We expect that LES will complement traditional dispersion modeling by providing: 1) the ability to discern between cases where traditional models work well and cases where more complicated characterizations are necessary, and 2) a method to investigate potentially unique flow features and turbulence structure for specific flow problems.

In the following, we present two cases where the unique features and turbulence structure have important implications for the dispersion. The first is neutral and stably stratified flow over a wavy lower boundary at the laboratory-scale, and the second is an atmospheric-scale stably stratified flow over a flat plain. In both of these cases, the particular turbulence structure varies dramatically either in space or time. For example, over the wavy boundary, the character of the turbulence over the troughs differs significantly from that over the crests. In the stratified flow over flat terrain, a turbulent bursting event varies the turbulence structure in time.

2. FLOW OVER A WAVY BOUNDARY

2.1 Setup and Methods

The basic grid configurations are similar to

that of a channel flow except that the bottom solid wall is deformed into the shape of the topography. In all the simulations, the flow is periodic in the streamwise and spanwise directions. The upper boundary is a solid no-slip wall.

The flows are driven with a constant pressure gradient and the Reynolds numbers based on mean velocity and total channel depths are approximately 7000. In the stably stratified case, the friction Richardson numbers were 31 and 62 (based on the density difference between fluid at the upper and lower boundaries, total depth, and a friction velocity derived from the driving pressure gradient). [See Calhoun and Street (1998) and Calhoun *et al.* (1998) for details.]

2.2 Flow Field

We have performed a number of simulations of flow over wavy topography; neutral cases with wavy bottom amplitudes, and several stably stratified cases. Full reports are available [Calhoun and Street, 1998; Calhoun *et al.*, 1998]. In this paper, we focus on the features of these flows which we believe are most relevant to dispersion modeling.

A large degree of variability exists in the instantaneous flow field. Compare the recirculation zones in Figure 1 and 2. The mean shows a smooth field with a small recirculation in the trough. Instantaneously, the recirculation may dominate the entire trough, be completely suppressed, or shift upstream/downstream. Computer animations of the developing flow field demonstrate that the trough region is frequently and vigorously 'scoured out' by turbulent structures.

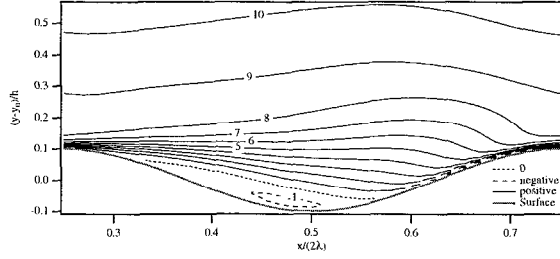


Figure 1. Mean streamwise velocity.

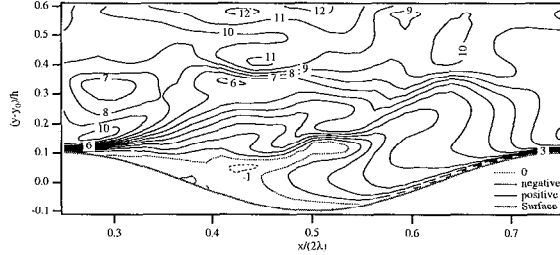


Figure 2. Instantaneous velocity vectors on a streamwise-vertical plane located at $z = 0.227L_z$.

The rate at which downstream-moving fluid sweeps out the recirculation zone is probably related to the detached shear layers that form in the lee of the crests (see Figure 3). Instability of the shear layer causes concentrations of vorticity ('rolling up') to appear. These roller vortices may impinge on the trough zone, the upslope portion of the wavy surface, or may be ejected into the free stream.



Figure 3. Spanwise vorticity on vertical-spanwise plane located at $z = 0.6L_z$.

The statistics of the turbulence over the wavy boundary would be difficult to accurately estimate without some knowledge of the fluid mechanical details of the flow. Figure 4, for example, shows the strong peak of mean turbulent kinetic energy located over the trough at approximately the height of the crests (for a wavy boundary amplitude equal to $1/20$ of the wavelength). The strength of the turbulence in this peak area is at least 4 times as strong as that near the downslope boundary and almost double that above the crests.

For an atmospheric flow which displayed this degree of heterogeneity in the turbulence field, the precise location of the release point of a toxic would be crucial in determining its short-term dispersion characteristics.

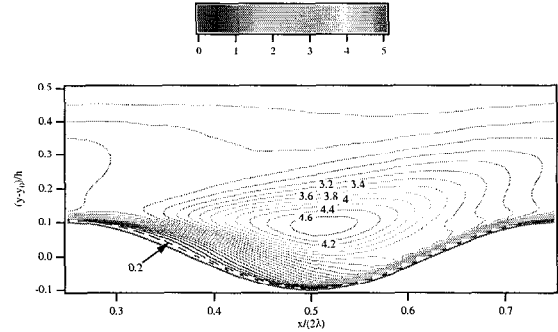


Figure 4. Mean turbulent kinetic energy nondimensionalized by u_*^2 .

These spatial relationships between the turbulence statistics and the wavy bottom boundary are dependent on hill height and level of stratification. In our laboratory examples, the mean TKE peak shifts downstream for lower amplitudes. It is not just the intensity of the turbulence that has a particular spatial relationship with the underlying topography; the type of turbulence, (for example, the level of anisotropy) is as well. This is demonstrated in Figures 5 and 6.

A decrease in the anisotropy parameter corresponds with a greater disparity between the scales of the vertical and horizontal turbulent intensities, and therefore a larger anisotropy. Notice that turbulence over the trough is more isotropic compared to that over the crest and near the upslope boundary. Therefore, a toxic cloud released over the trough would (in addition to being mixed strongly) be mixed more uniformly than a release near the upslope or crest regions.

Notice that as the flow becomes increasingly stratified (Figure 5 to Figure 6) and fluid motion in the vertical direction is depressed, anisotropy increases. The trend of increasing anisotropy in more stratified flows and the widely varying levels of anisotropy in complex flows provides strong evidence that more detailed turbulence assumptions and input may be necessary for accurate dispersion modeling of complicated scenarios.

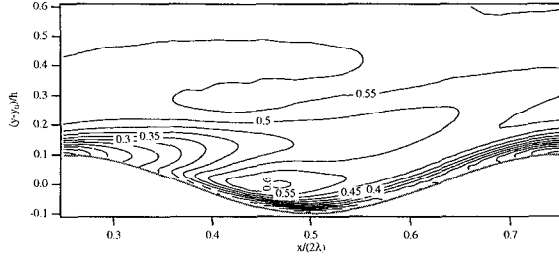


Figure 5. Anisotropy parameter V_{rms}/U_{rms} . Case $Ri_\tau = 31$.

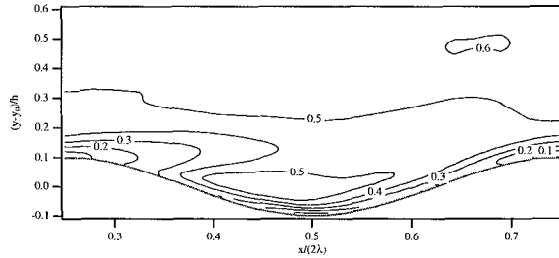


Figure 6. Anisotropy parameter V_{rms}/U_{rms} . Case $Ri_\tau = 62$.

We summarize this section by showing Figure 7 which displays an iso-surface of a passive scalar diffusing into the flow field from the lower wavy boundary. Notice that the surface is much more varied (and isotropic) over the trough regions. In addition, riblets or streamwise indentations can be seen in the surface connecting the trough areas. These are the result of streamwise vortices which are locked into a particular phase relationship with the underlying topography. For more information on streamwise vortices over wavy topography see Calhoun and Street (1999).

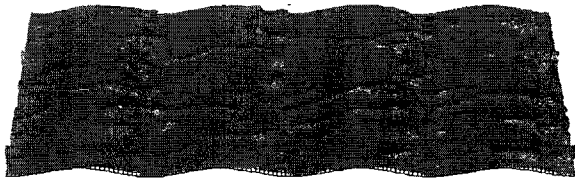


Figure 7. Iso-contours of temperature.

3. STABLE BOUNDARY LAYER

Results from large-eddy simulation (LES) of the atmospheric boundary layer can be used to evaluate the transport and dispersion under stable and unstable atmospheric conditions. Impact assessments usually treat the stable boundary layer (SBL) as the worst case scenario, so we

will concentrate here on LES results for an SBL case. The LES techniques that we use are able to resolve fine-scale features of the flow, and the associated spatially and temporally varying and intermittent turbulence. Traditional Reynolds-averaging approaches for turbulence used in most air pollution models are not well suited for unsteady turbulence in the SBL.

The simulations address the transition from the convective boundary layer (CBL) that develops during the afternoon to the SBL that develops after sunset. In the CBL, turbulent transport comes primarily from large, thermally-driven eddies that develop in response to surface heating. As the surface heating is replaced by surface cooling after sunset, the CBL collapses. The much-reduced turbulent transport comes from shallow, shear-driven eddies. In simulations using a previous SGS model, the collapse of the CBL was too rapid (Cederwall, 1995). Our advanced SGS model allows the backscatter (upscale transfer) of energy that provides a more realistic simulation of the evolving SBL (Cederwall and Street, 1997).

3.1 Setup and Methods

Our LES model is based on one used previously for atmospheric boundary layer studies (Wyngaard and Brost, 1984; Nieuwstadt and Brost, 1986). A second-order accurate leapfrog scheme is used for time integration; the scheme is also non-dissipative and employs a time filter to control the computational modes. The value of the damping factor was reduced to 0.1 from 0.02 to minimize the impact on the fine-scale velocity. A second-order accurate scheme is used for advection that conserves velocity variance (Piacsek and Williams, 1970). The advection scheme has very little numerical diffusion, so a 4th order dissipation term was added to control for non-linear instabilities.

The subgrid scale (SGS) is a two-parameter approach that dynamically evaluates coefficients for the eddy viscosity and the modified Leonard term, and allows backscatter (upscale transfer) of energy (Cederwall and Street, 1997, 1999). The SGS model uses a time-evolving SGS turbulent kinetic energy (TKE) scheme (Deardorff, 1980) so that effects of atmospheric stability and turbulent transport of SGS TKE can be incorporated. Corresponding dynamic equations are developed for SGS heat flux.

The momentum forcing at the top of the

model is a constant geostrophic wind of 10.4 m/s. A weak temperature inversion is initially prescribed at the upper fourth of the model levels. Similarity is used at the bottom boundary, with a roughness length of 10 cm. The grid resolution for these simulations was 20 m in the horizontal and 5 m in the vertical. The prescribed surface heat flux for the CBL is 0.06 Km/s (75 W/m²). The surface heat flux is then decreased linearly over a 1-hour period to -0.02 Km/s (-25 W/m²) to represent the period around sunset. The surface flux then remains constant during the rest of the simulation as the SBL develops.

3.2 Flow Field

The simulated SBL is characterized by strong vertical gradients of horizontal wind speed and direction. Hence, the transport of material in the SBL depends critically on height. To explore this, we simulated the release marker particles into the simulated wind fields.

The methodology for simulating the release and resulting dispersion is straight forward. The release scenario was a collection of 75 marker particles released every second and tracked to illustrate the different transport and dispersion features of the simulated flows. The particles were advanced with a one-second time step. The transport wind was determined by trilinear interpolation of values at the corners of the volume containing the particle. Almost all of the velocity variance is resolved, except very near the ground, so no additional perturbation is added to the transport velocity to account for SGS turbulence.

The release positions were centered on a specified release point, with 5 positions in each of the horizontal directions equally spaced across 10 m, and repeated 3 times in the vertical direction, equally spaced across 1 m. The release duration was 5 minutes, giving a population of 22,500 particles for each release. After some time, particles were transported horizontally beyond the model grid. The use of periodic boundary conditions allowed us to handle this situation, as was done by Kemp and Thomson (1996).

In our SBL simulations, we had an event when the turbulence was enhanced. The vertical profiles of velocity variance show the increased levels of turbulence in the horizontal wind components (see Figure 8). To evaluate how dispersion would be altered by the enhanced turbulence event, we simulated the release of material at five heights (10

m, 30 m, 50 m, 70 m, and 90 m). The resulting simulated plumes are shown in Figure 9 for the period before the event in Figure 9. Note that the vertical scale is much smaller than the horizontal scale in the figures. The height dependence of speed and direction of transport is clearly evident. There is not a strong variation in dispersion with height.

The location of marker particles released during the enhanced turbulence event tells a different story. Within the middle portion of the SBL, there is much greater dispersion, as seen in Figure 10. This leads to significantly reduced concentration of released material which can be estimated from the marker particles, as done by Kemp and Thomson (1996), but greater spatial coverage. For toxic materials, the concentration levels and spatial coverage are important, since transient exposures can lead to health impacts even when the long-term average concentrations are below health effect levels.

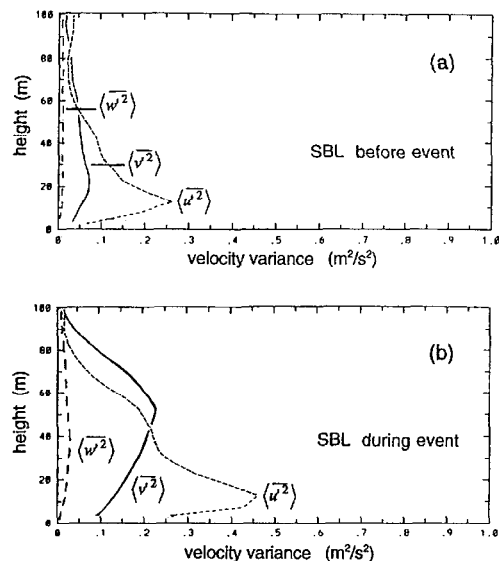


Figure 8. Vertical profiles of velocity variance (a) before and (b) during the enhanced turbulence event in the SBL.

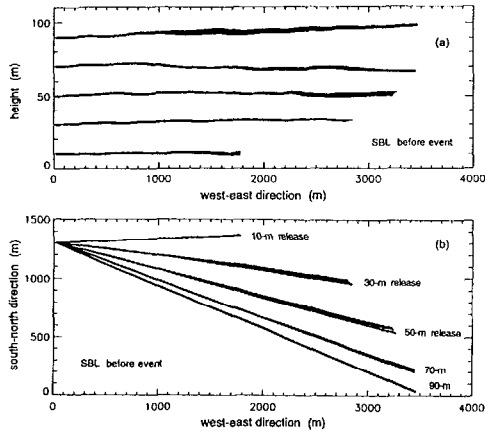


Figure 9. Location of marker particles for 5-minute release before SBL event in (a) x-z plane, and (b) x-y plane.

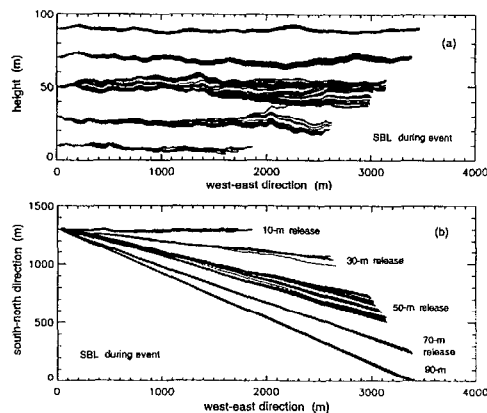


Figure 10. Location of marker particles for 5-minute release during SBL event in (a) x-z plane, and (b) x-y plane.

4. SUMMARY

We have presented two flows where detailed knowledge of the fluid mechanics would appear to be crucial for accurate dispersion modeling. We expect that LES will complement traditional dispersion modeling by providing both the ability to discern between cases where traditional models work well and cases where more complicated characterizations are necessary, and a method to investigate potentially unique flow features and turbulence structure for specific flow problems.

Acknowledgment

The above research was a LLNL/Stanford collaboration supported by the U.S. Department of Energy at the Lawrence Livermore National Laboratory under contract number W-7405-Eng-48 and by NSF grant ATM-9526246 and ONR grant N00014-94-0190 at Stanford University.

BIBLIOGRAPHY

Calhoun, R., and Street, R. 1999 Vortical structures in flow over topography: an LES at laboratory-scale. *13th Symp. on Boundary Layers and Turbulence, AMS. Boston*, 227-230.

Calhoun, R., and Street, R. 1998 Turbulent flow over a wavy surface: Part 1: Neutral case. *Journal of Geophysical Research. Submitted*.

Calhoun, R., Street, R., and Koseff, J. 1998 Turbulent flow over a wavy surface: Part 2: Stratified case. *Journal of Geophysical Research. Accepted*.

Cederwall, R. 1995 Large-eddy simulation of the development of stably-stratified atmospheric boundary layers over cool flat surfaces. *11th Symp. Boundary Layers and Turbulence, AMS. Charlotte, NC*, 572-575.

Cederwall, R., Street, R. 1997 Use of a dynamic subgrid-scale model for large-eddy simulation of the planetary boundary layer. *12th Symp. Boundary Layers and Turbulence, AMS. Vancouver, BC*, 215-216.

Cederwall, R., Street, R. 1999 Turbulence modification in the evolving stable boundary layer: a large-eddy simulation. *13th Symp. on Boundary Layers and Turbulence, AMS. Boston*, 223-226.

Deardorff, J. 1980 Stratocumulus-capped mixed layers derived from a three-dimensional model. *Bound.-Layer Meteorol.* **18**, 595-627.

Kemp, J., Thomson, T. 1996 Dispersion in stable boundary layers using large-eddy simulation. *Atmos. Environ.* **30**, 2911-2923.

Nieuwstadt, F., Brost, R. 1986 The decay of convective turbulence. *J. Atmos. Sci.* **43**, 532-546.

Piacsek, S., Williams, G. 1970 Conservation properties of convection difference schemes. *J. Comput. Phys.* **6**, 392-405.

Wyngaard, J., Brost, R. 1984 Top-down and bottom-up diffusion of a scalar in the convective boundary layer. *J. Atmos. Sci.* **41**, 102-112.